Laser-ranging long-baseline differential atom interferometers for space

Sheng-wey Chiow, Jason Williams, and Nan Yu[*]

Jet Propulsion Laboratory, California Institute of Technology, Pasadena, California 91109, USA
(Received 19 February 2015; published 7 December 2015)

High-sensitivity differential atom interferometers (AIs) are promising for precision measurements in science frontiers in space, including gravity-field mapping for Earth science studies and gravitational wave detection. Difficulties associated with implementing long-baseline differential AIs have previously included the need for a high optical power, large differential Doppler shifts, and narrow dynamic range. We propose a configuration of twin AIs connected by a laser-ranging interferometer (LRI-AI) to provide precise information of the displacements between the two AI reference mirrors and also to phase-lock the two independent interferometer lasers over long distances, thereby drastically improving the practical feasibility of long-baseline differential AI measurements. We show that a properly implemented LRI-AI can achieve equivalent functionality to the conventional differential AI measurement configuration.

I. INTRODUCTION

Atom interferometry exploits the wave nature of neutral atoms for precision metrology: The wave property allows each atom to interfere with itself, resulting in modulation of the probability of populating a discrete state, associated with the environment that the atom traverses [1]. In a light-pulse atom interferometer (AI), an atomic matter wave is split, reflected, and recombined by laser pulses, and during each pulse the optical phase is registered by the atom. The output phase of the AI, the probability distribution among possible states, depends on the optical phases and the evolution of the atomic wave under the influences of environmental perturbations, including electromagnetic fields, gravity, etc. Due to the inherent stability and identicality of atomic properties for the same species, the accuracy of an AI is fundamentally limited by the stability of the interrogating laser and the understanding and control of the environment. This is in contrast to classical sensors, which drift over time and possess bulk effects that depend on their shape and composition. The repeatability and thorough understanding of atomic systems make cold-atom-based instruments ideal candidates for precision measurements, including local gravity acceleration g [2], photon recoil measurement of $\hbar/m$ and the fine structure constant α [3], rotation [4], and the gravitational constant G [5,6]. The power of AI-based precision measurements is illustrated in Ref. [2]: An AI gravimeter not only surpasses the short-term sensitivity of a state-of-the-art classical falling corner cube gravimeter, but also agrees with global and regional gravity models over 4 years, thus restricting local Lorentz variance in gravity and electromagnetism to unprecedented levels.

The applicability of atom interferometry is further extended by a widely used technique, differential measurements between two simultaneous AIs [7–10] as depicted in Fig. 1(a). In this scheme, two AIs are interrogated by a common laser, using either the same or different spectral components of the beam [9]. The instrument sensitivity increases proportionally to the baseline, while the contribution of baseline uncertainty to measurement error decreases. The vibrations of optics in

the laser beam path, as well as the laser phase noise, are largely common to the two AIs, thanks to the relatively short propagation delay for a laser pulse to go from one AI to the other [11]. Common mode noise suppression of vibrations is demonstrated to exceed 140 dB [12]. Differential measurements allow instrument sensitivity beyond the abilities to control and quantify systematic errors of individual AIs. In particular, AI gravity gradiometers [5,6,10,13] are constructed for terrestrial and space-oriented applications. Furthermore, spaceborne gravitational wave detection using differential AIs are proposed for frequency bands and sensitivities unachievable on Earth [14–17].

As the instrument baseline L increases for demanding sensitivity requirements, however, associated technical challenges may become prohibitively expensive to overcome for the conventional configuration, if at all possible. For instance, as discussed in detail in [15], the Rayleigh range $z_R = \pi w_0^2/\lambda$ of a Gaussian beam with waist w_0 and wavelength λ should be larger than L to efficiently deliver optical power from one site to the other, $2z_R \geqslant L$. Thus a longer baseline demands a larger beam waist, $w_0 \propto \sqrt{L}$, and, correspondingly, bigger high-quality optics. Similarly, the laser power required to maintain the same intensity at z_R for AIs is proportionally higher. Moreover, if the twin AIs are hosted inside one single vacuum chamber, the baseline is limited to $\ll 1$ km even with the help of a boom system [16]. In the configuration where twin AIs are housed in different spacecraft with the common laser passing through free space using complex optics systems, static and stochastic wavefront aberrations may be of serious concern [18,19].

II. THE LRI-AI CONFIGURATION

Here we propose an alternative approach for differential AI measurements, which drastically improves the practical feasibility of long-baseline differential AIs. As depicted in Fig. 1(b), instead of a common interrogation laser for both AIs, our approach is constituted of twin local AIs driven by independent lasers and a laser-ranging interferometer (LRI) to link the AIs (LRI-AI). A similar concept using independent AIs for gravitational wave detection was previously proposed [20].
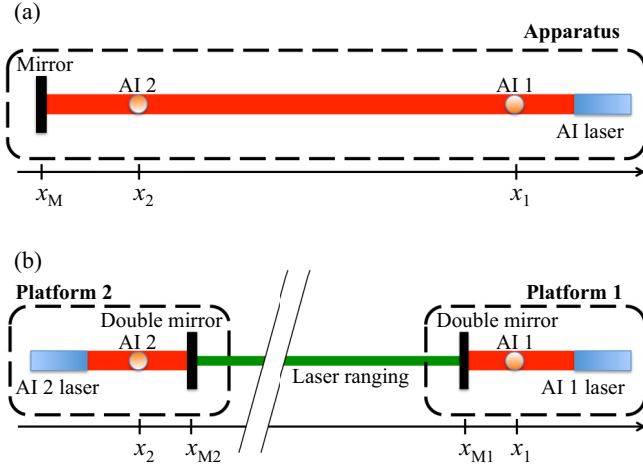
———————
[*]nan.yu@jpl.nasa.gov

FIG. 1. (Color online) (a) Conventional differential AIs hosted in one apparatus. x_i is the position of the corresponding element. The instrument baseline $L = x_1 - x_2$. (b) Twin AIs linked with a laser-ranging interferometer (LRI-AI). The double mirror has a reflective surface serving as the retroreflection mirror for the AI on one side and serving as the retroreflection mirror for the LRI on the other side.

Conceptually, the LRI-AI can be pictured as using phase-locked lasers to replace the common laser in the conventional differential AI configuration, thus the fundamental measurement concept is the same for both: atomic motions are interrogated by a coherent classical light field. In a conceptual dual-AI arrangement, the readout phase of a Mach-Zehnder AI is $\psi_i = k_{\text{eff}_i}(\ddot{x}_i - \ddot{x}_{Mi})T^2 + \phi_{li}$, where $i = (1,2)$, k_{eff} is the effective wave number, T the pulse separation time, and x_{Mi} and ϕ_{li} indicate the mechanical reference point and the combination of AI laser phases. The differential acceleration experienced by the two atomic ensembles is revealed by taking the phase difference:

$$\psi_1 - \psi_2 = \left(k_{\text{eff}_1}\ddot{x}_1 - k_{\text{eff}_2}\ddot{x}_2\right)T^2$$
$$- (k_{\text{eff}_1}\ddot{x}_{M1} - k_{\text{eff}_2}\ddot{x}_{M2})T^2 + (\phi_{l1} - \phi_{l2}).$$

In the conventional configuration [Fig. 1(a)], both AIs share a single AI laser and a common mechanical reference point, thus k_{eff_i}, $\ddot{x}_{Mi}$, and ϕ_{li} are common (neglecting the propagation delay). $\delta\psi = \psi_1 - \psi_2 = k_{\text{eff}}(\ddot{x}_1 - \ddot{x}_2)T^2$, with both the mechanical acceleration and the laser phase noise terms canceled out [7,8]. In the LRI-AI [Fig. 1(b)], x_{M1} and x_{M2} are different, but the LRI provides $\ddot{L} = \ddot{x}_{M1} - \ddot{x}_{M2}$ measurement. The combination

$$\psi_1 - \psi_2 + k_{\text{eff}}\ddot{L}T^2 = k_{\text{eff}}(\ddot{x}_1 - \ddot{x}_2)T^2 \qquad (1)$$

yields a differential phase identical to that of the conventional configuration, provided that k_{eff_i} and laser phases are precisely known. Note that the positions x_{Mi} of the retroreflection mirrors drop out of the differential measurement as expressed in Eq. (1) and need not be actively controlled.

It is not always necessary to phase-lock AI lasers to the ranging laser, as in the conceptual picture, to establish the equivalence to the conventional configuration, where the purpose of phase-locking is to remove differential k_{eff} and laser phase noise in ϕ_l. For a conventional AI using counter-propagating Raman or Bragg beams, as opposed to those using single-photon beam splitters proposed in [14] and [17], the laser phase noise in the AI measurement ϕ_i is determined by the relative phase noise between the counter-propagating beams, i.e., the phase noise of the radio-frequency source that generates the counter-propagating beams [23]. Thus, a sufficiently low uncertainty of k_{eff} and laser phase ϕ_l beyond the fundamental noise floor (such as atom shot noise) can be guaranteed without such phase-lock. For instance, with an assumed AI phase resolution of 1 mrad and $T \sim 1$ s for Earth gravity measurements, the requirement on the local oscillator is ~ -60 dBc/Hz in phase noise, or $\sim 1 \times 10^{-13}$ frequency stability at 1 s for a 10-GHz local oscillator. Existing ultrastable oscillators can provide such noise performance. Similarly, sufficient knowledge of the acceleration sensitivity coefficient $k_{\text{eff}}T^2$ is easily achieved, where the requirement on its accuracy is the same as in the conventional configuration. Without the need for phase-locking, the ranging laser can have very different wavelengths from AI lasers, thus making the LRI-AI easily integrable to existing implementations, as proposed for gravitational wave detection [20]. For very long baselines such that propagation delay is not negligible for the stability of the ranging laser, variations of the time-delay interferometer can be used [14,24,25].

III. COMPARISON OF THE LRI-AI WITH THE CONVENTIONAL AI SCHEME

The LRI-AI is advantageous over the conventional configuration in several aspects. First, LRI technology is well developed in GRACE-FO for Earth gravity measurements [21] and in LISA for gravitational wave detection [26]. The LRI-AI does not impose more stringent requirements on the ranging laser than already developed, because the ranging laser is used only to deliver the phase information such that a small amount of the received laser power ($<$nW) is sufficient, where beam collimation and wavefront aberrations are not critical either. Mitigating the otherwise required large AI laser beam size for delivering the beam over a long distance, local AI laser beams in the LRI-AI can be tailored for the local atomic sample size, optimization, and systematic control. A higher intensity for large-momentum-transfer beam splitters will also be more affordable in the LRI-AI [27–31]. Furthermore, one of the operational difficulties of using a common laser for two spacecraft-based AIs is to accommodate the relative Doppler shift between distant spacecraft, which can be of the order of megahertz [21] and may prevent simultaneous operation of distant AIs using a single common laser without a further mitigation strategy. In the LRI-AI configuration, local AIs are relatively stationary to the spacecraft, while the large Doppler shift is registered by heterodyne measurements in the LRI [21].

The LRI-AI is readily implementable, with compelling performance, by adopting mature technologies in the LRI and compact AI, in comparison to the extensive technology development and validation effort for the conventional long-baseline AI configuration for space applications. AI-based measurements are fundamentally limited by atom shot noise, and we argue that LRI technology maturity [21,26] can support an atom-shot-noise-limited LRI-AI with a baseline >100 km, of which the feasibility is rather questionable in the

TABLE I. Performance of LRI-AI using demonstrated technologies. While conventional differential AIs will be limited by AI sensitivity only, LRI-AI performance will also be limited by AI sensitivity at frequencies $f < 0.1$ Hz for thermal AIs and at frequencies $f < 0.01$ Hz for BEC AIs.

Atom source	AI interrogation time T (s)	AI acceleration sensitivity (nm/s^2/$\sqrt{\text{Hz}}$)	LRI ranging sensitivity (nm/$\sqrt{\text{Hz}}$)	LRI acceleration sensitivity (nm/s^2/$\sqrt{\text{Hz}}$)
Thermal AI	0.16 [6]	30 [6]	80 [21]	$31.6 \times (f/0.1)^2$
BEC AI	1.15 [22]	0.3 [22]	80 [21]	$31.6 \times (f/0.1)^2$

conventional configuration. Table I summarizes hypothetical combinations of LRI and AIs demonstrated to date, based on the LRI development for GRACE-FO [21] and state-of-the-art terrestrial AIs [6,22]. It is clear that an LRI system similar to that developed for GRACE-FO, with a baseline up to 270 km, including the expected influences of thermal, acoustic, and vibrational effects on the optical path length, would have the same AI-limited performance as conventional differential AIs at time scales longer than 10 s for thermal sources and at time scales longer than 100 s for BEC sources, while the technology for such long-baseline AIs in the conventional configuration is still under development. For the LRI to support AIs at shorter time scales, advanced LRIs can be adapted such as that demonstrated for the LISA mission, with $1000\times$ better performance [21]. Indeed, the current LRI can support state-of-the-art AIs, which is, at best, what a conventional AI configuration can achieve.

IV. IMPLEMENTATION OF THE LRI-AI

As an example to illustrate the power of the LRI-AI, a combination of a terrestrial-demonstrated thermal AI and the GRACE-FO LRI with a baseline of 200 km will have a gravity gradient sensitivity of 150 μE/$\sqrt{Hz}$ [E (Eötvös) = $10^{-9}/s^2$], which compares favorably to the gradiometers of ~ 1 mE/$\sqrt{Hz}$ in GOCE [32]. The achievable sensitivity can be further enhanced with the use of BEC sources and longer T's available under microgravity. Again, using the demonstrated BEC AI sensitivity and a baseline of 200 km, one can achieve 1.5 μE/$\sqrt{Hz}$. Such a gravity gradient measurement system is expected to improve on the current GRACE gravity measurement significantly, though detailed gravity recovery simulation is required for its ability to recover gravity through gradient measurements. In addition to improved sensitivity, the LRI-AI also provides atomic-clock-grade stability, which is lacking in current gravity missions. Uncertainty in the scale factor calibration and variations associated with the mechanical accelerometers used in GRACE and GOCE are potential error sources. On the other hand, the AI technique has demonstrated unprecedented long-term stability [2,4].

The LRI-AI also mitigates systematics in gravity measurements associated with the self-gravity gradient (SG) of spacecraft. The SG influences accelerometers onboard depending on the relative position of the spacecraft and the test mass, and thus generates error in acceleration measurements. To completely remove the spacecraft SG error, the spacecraft can fly drag-free, similar to the GOCE or LISA mission concept, where the spacecraft is servoed to follow the free-falling test mass using thrusters. However, at a lower Earth orbit altitude drag-free flight is difficult and has a very limited mission

lifetime due to fuel consumption. On the other hand, in the LRI-AI approach, the atoms on each platform will serve as ideal drag-free references in the presence of the spacecraft SG when the interrogation time is kept relatively short, which renders drag-free flight unnecessary [33].

Current methods of differential phase extraction between AIs rely on the constancy of the phase difference and high common mode rejection [7,8] during stationary data acquisition in a laboratory environment. This requirement reduces the spatial-temporal resolution of an instrument in a dynamic moving platform such as in low Earth orbit, where actual common phase AIs are unpredictable and random. The situation in the LRI-AI may appear to be worse in that the phase difference between AIs also depends on the motion of the local inertial reference point; there is no commonality of the motions for the two inertial reference points on different spacecraft. A mitigation unique to the LRI-AI scheme can be implemented that greatly enhances the useful data rate (Fig. 2): Each local AI is operated near a phase zero crossing (equal probability between two output ports) by controlling the AI beam-splitter phase based on the reading of a mechanical accelerometer [34,35]. In this scheme, the mechanical accelerometer provides an estimate of the mirror acceleration, allowing AI laser phase adjustment to compensate for the anticipated phase excursion so as to maintain a near-zero readout phase. The error of the estimate will manifest as the AI readout phase. After the AI completes, combining the AI phase and the applied phase adjustment gives a highly accurate and stable acceleration measurement of the reflection mirror relative to the freefall atoms, with a greatly extended dynamic range of
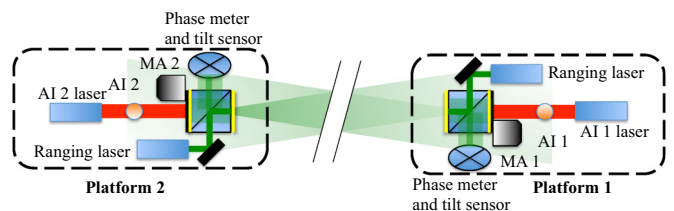

FIG. 2. (Color online) Schematic of the LRI-AI with key components. Local forces measured by a mechanical accelerometer (MA) are used to feed back on the AI laser phase to compensate for excessive excursions of the retroreflection surface and thus to maintain the AI phase near 0, where the sensitivity is optimal. Ranging beams are circularly polarized with the quarter wave plates (yellow plates) after polarization beam-splitting cubes. The beat note between local and remote lasers is obtained after the remote beam is reflected off the back of the AI mirror (double-passing a quarter wave plate) and directed to the phase meter by the polarization beam-splitting cube. Relative tilt can be read off from the quadrant detector [21].

mechanical accelerometers. The AI differential phase can be easily calculated while the LRI provides satellite ranging with a high stability and sensitivity to accommodate shot-to-shot variation of the differential signal, including Doppler shifts of the order of megahertz.

V. CONCLUSION

In summary, we propose a new method for long-baseline atom interferometers (AIs) with laser ranging in space. This method adapts the state-of-the-art accurate atomic accelerometer technology and the technical advancement of laser-ranging interferometry, allowing >100-km-baseline differential AIs with a low optical power and a compact apparatus. With the assistance of mechanical accelerometers to keep the AIs

operating at their most sensitive phase points, the LRI-AI exhibits a large dynamic range, fast data extraction, and low aliasing for high-resolution spatial-temporal mapping. This method will be applicable in AI-based spaceborne gravity measurements as well as in gravitational wave detection.

Note added in proof. Recently, we became aware of the paper by Hogan *et al.* discussing a similar configuration [36].

ACKNOWLEDGMENTS

[1] A. D. Cronin, J. Schmiedmayer, and D. E. Pritchard, Optics and interferometry with atoms and molecules, Rev. Mod. Phys. **81**, 1051 (2009).

[2] K.-Y. Chung, S.-w. Chiow, S. Herrmann, S. Chu, and H. Müller, Atom interferometry tests of local Lorentz invariance in gravity and electrodynamics, Phys. Rev. D **80**, 016002 (2009).

[3] R. Bouchendira, P. Cladé, S. Guellati-Khélifa, F. Nez, and F. Biraben, New Determination of the Fine Structure Constant and Test of the Quantum Electrodynamics, Phys. Rev. Lett. **106**, 080801 (2011).

[4] J. K. Stockton, K. Takase, and M. A. Kasevich, Absolute Geodetic Rotation Measurement Using Atom Interferometry, Phys. Rev. Lett. **107**, 133001 (2011).

[5] J. B. Fixler, G. T. Foster, J. M. McGuirk, and M. A. Kasevich, Atom interferometer measurement of the Newtonian constant of gravity, Science **315**, 74 (2007).

[6] M. Prevedelli, L. Cacciapuoti, G. Rosi, F. Sorrentino, and G. M. Tino, Measuring the Newtonian constant of gravitation G with an atomic interferometer, Philos. Trans. A Math. Phys. Eng. Sci. **372**, 2026 (2014).

[7] G. T. Foster, J. B. Fixler, J. M. McGuirk, and M. A. Kasevich, Method of phase extraction between coupled atom interferometers using ellipse-specific fitting, Opt. Lett. **27**, 951 (2002).

[8] J. K. Stockton, X. Wu, and M. A. Kasevich, Bayesian estimation of differential interferometer phase, Phys. Rev. A **76**, 033613 (2007).

[9] S.-w. Chiow, S. Herrmann, S. Chu, and H. Müller, Noise-Immune Conjugate Large-Area Atom Interferometers, Phys. Rev. Lett. **103**, 050402 (2009).

[10] N. Yu, J. Kohel, L. Romans, and L. Maleki, Quantum gravity gradiometer sensor for earth science applications, in *NASA Earth Science and Technology Conference 2002, Pasadena, California* (2002), p. B3P5.

[11] J. Le Gouët, P. Cheinet, J. Kim, D. Holleville, A. Clairon, A. Landragin, and F. Pereira Dos Santos, Influence of lasers propagation delay on the sensitivity of atom interferometers, Eur. Phys. J. D **44**, 419 (2007).

[12] J. M. McGuirk, G. T. Foster, J. B. Fixler, M. J. Snadden, and M. A. Kasevich, Sensitive absolute-gravity gradiometry using atom interferometry, Phys. Rev. A **65**, 033608 (2002).

[13] N. Yu, J. M. Kohel, J. R. Kellogg, and L. Maleki, Development of an atom-interferometer gravity gradiometer for gravity measurement from space, Appl. Phys. B **84**, 647 (2006).

[14] N. Yu and M. Tinto, Gravitational wave detection with single-laser atom interferometers, Gen. Relativ. Grav. **43**, 1943 (2011).

[15] S. Dimopoulos, P. W. Graham, J. M. Hogan, M. A. Kasevich, and S. Rajendran, Atomic gravitational wave interferometric sensor, Phys. Rev. D **78**, 122002 (2008).

[16] J. M. Hogan, D. M. S. Johnson, S. Dickerson, T. Kovachy, A. Sugarbaker, S.-w. Chiow, P. W. Graham, M. A. Kasevich, B. Saif, S. Rajendran, P. Bouyer, B. D. Seery, L. Feinberg, and R. Keski-Kuha, An atomic gravitational wave interferometric sensor in low earth orbit (AGIS-LEO), Gen. Relativ. Grav. **43**, 1953 (2011).

[17] P. W. Graham, J. M. Hogan, M. A. Kasevich, and S. Rajendran, New Method for Gravitational Wave Detection with Atomic Sensors, Phys. Rev. Lett. **110**, 171102 (2013).

[18] P. L. Bender, Comment on "Atomic Gravitational Wave Interferometric Sensor," Phys. Rev. D **84**, 028101 (2011).

[19] S. Dimopoulos, P. W. Graham, J. M. Hogan, M. A. Kasevich, and S. Rajendran, Reply to "Comment on 'Atomic Gravitational Wave Interferometric Sensor,'" Phys. Rev. D **84**, 028102 (2011).

[20] N. Yu, M. Tinto, J. M. Kohel, and R. J. Thompson, Drag-free atomic acceleration reference for LISA disturbance reduction system, *Submission to the NASA RFI: Concepts for the NASA Gravitational Wave Mission (http://pcos.gsfc.nasa.gov/studies/gravwave/gravitational-wave-mission-rfis.php)* (2011).

[21] B. S. Sheard, G. Heinzel, K. Danzmann, D. A. Shaddock, W. M. Klipstein, and W. M. Folkner, Intersatellite laser ranging instrument for the GRACE follow-on mission, J. Geodesy **86**, 1083 (2012).

[22] S. M. Dickerson, J. M. Hogan, A. Sugarbaker, D. M. S. Johnson, and M. A. Kasevich, Multiaxis Inertial Sensing with Long-Time Point Source Atom Interferometry, Phys. Rev. Lett. **111**, 083001 (2013).

[23] P. Cheinet, B. Canuel, F. Pereira Dos Santos, A. Gauguet, F. Yver-Leduc, and A. Landragin, Measurement of the sensitivity

function in a time-domain atomic interferometer, IEEE Trans. Instrument. Measure. **57**, 1141 (2008).

[24] M. Tinto and S. V. Dhurandhar, Time-delay interferometry, Living Rev. Relativ. **8**, 4 (2005).

[25] G. de Vine, B. Ware, K. McKenzie, R. E. Spero, W. M. Klipstein, and D. A. Shaddock, Experimental Demonstration of Time-Delay Interferometry for the Laser Interferometer Space Antenna, Phys. Rev. Lett. **104**, 211103 (2010).

[26] P. Bender, *LISA: Laser Interferometer Space Antenna for the Detection and Observation of Gravitational Waves: Pre-phase A Report* (Max-Planck-Institut fur Quantenoptik, Garching, Germany, 1998).

[27] S.-w. Chiow, T. Kovachy, H.-C. Chien, and M. A. Kasevich, $102\hbar k$ Large Area Atom Interferometers, Phys. Rev. Lett. **107**, 130403 (2011).

[28] H. Müller, S.-w. Chiow, Q. Long, S. Herrmann, and S. Chu, Atom Interferometry with up to 24-Photon-Momentum-Transfer Beam Splitters, Phys. Rev. Lett. **100**, 180405 (2008).

[29] J. M. McGuirk, M. J. Snadden, and M. A. Kasevich, Large Area Light-Pulse Atom Interferometry, Phys. Rev. Lett. **85**, 4498 (2000).

[30] H. Müller, S.-w. Chiow, and S. Chu, Atom-wave diffraction between the Raman-Nath and the Bragg regime: Effective Rabi frequency, losses, and phase shifts, Phys. Rev. A **77**, 023609 (2008).

[31] S. S. Szigeti, J. E. Debs, J. J. Hope, N. P. Robins, and J. D. Close, Why momentum width matters for atom interferometry with Bragg pulses, New J. Phys. **14**, 023009 (2012).

[32] J. A. Johannessen, G. Balmino, C. Le. Provost, R. Rummel, R. Sabadini, H. Sünkel, C. C. Tscherning, P. Visser, P. Woodworth, C. Hughes, P. Legrand, N. Sneeuw, F. Perosanz, M. Aguirre-Martinez, H. Rebhan, and M. Drinkwater, The European gravity field and steady-state ocean circulation explorer satellite mission its impact on geophysics, Surv. Geophys. **24**, 339 (2003).

[33] The drag-free aspect of atoms does not guarantee complete immunity to SG. Even though atoms are in free fall during the AI interrogation time, motion of the spacecraft about the atoms during this time gives an uncertainty to the influence of the spacecraft self-gravity that can manifest as systematic and statistical noise sources. The typical drag for the GRACE-FO mission, assuming a 225-km altitude orbit, corresponds to ≈ 16 μm/s^2 and fluctuates by $\approx 25\%$ per cycle [37]. For a reasonable magnitude of the SG on a GRACE-like spacecraft, 10^{-6}m/s^2 over a 1-m baseline, the error of the AI due to the combination of drag and SG is $\approx 8 \pm 2 \times 10^{-12}$ m/s$^2(T/s)^2$. This error has significant ramifications for the drag-free constraints of our AI-based mission concepts. At $T = 10$ s, the SG error approaches 10^{-10}m/s^2 and quickly dominates at higher sensitivities. In fact, we conclude that we can only allow for $T \sim 1$ s to avoid significant SG error in low Earth orbit without using drag-free satellites. For gravitational wave detection, the spacecraft SG will be a severe limitation. To mitigate this limitation, atoms away from spacecraft masses have been proposed [17, 20].

[34] N. Yu and L. Maleki, Atomic references for measuring small accelerations, *NASA Technical Briefs*, March 2009, 30 (2009).

[35] J. Lautier, L. Volodimer, T. Hardin, S. Merlet, M. Lours, F. Pereira Dos Santos, and A. Landragin, Hybridizing Matter-Wave and Classical Accelerometers, Appl. Phys. Lett. **105**, 144102 (2014).

[36] J. M. Hogan and M. A. Kasevich, Atom interferometric gravitational wave detection using heterodyne laser links, arXiv:1501.06797.

[37] J. Blandino, M. Demetriou, and N. Gatsonis, *Analysis of Drag-Free Spacecraft Motion and Control in Low Earth Orbit, Technical Report* (Worchester Polytechnic Institute, Worchester, MA, 2006).